

Margin-Based Regularization and Selective Sampling in Deep Neural Networks

Berry Weinstein,¹ Shai Fine,² Yacov Hel-Or¹

¹ Efi Arazi School of Computer Science, Interdisciplinary Center, Herzliya, Israel

² The Data Science Institute, Interdisciplinary Center, Herzliya, Israel
berry.weinstein@post.idc.ac.il, shai.fine@idc.ac.il, toky@idc.ac.il

Abstract

We derive a new margin-based regularization formulation, termed *multi-margin regularization* (MMR), for *deep neural networks* (DNNs). The MMR is inspired by principles that were applied in margin analysis of shallow linear classifiers, e.g., *support vector machine* (SVM). Unlike SVM, MMR is continuously scaled by the radius of the bounding sphere (i.e., the maximal norm of the feature vector in the data), which is constantly changing during training. We empirically demonstrate that by a simple supplement to the loss function, our method achieves better results on various classification tasks across domains. Using the same concept, we also derive a selective sampling scheme and demonstrate accelerated training of DNNs by selecting samples according to a *minimal margin score* (MMS). This score measures the minimal amount of displacement an input should undergo until its predicted classification is switched. We evaluate our proposed methods on three image classification tasks and six language text classification tasks. Specifically, we show improved empirical results on CIFAR10, CIFAR100 and ImageNet using state-of-the-art *convolutional neural networks* (CNNs) and BERT_{BASE} architecture for the MNLI, QQP, QNLI, MRPC, SST-2 and RTE benchmarks.

1 Introduction

Over the last decade, deep neural networks (DNNs) have become the *machine learning* method of choice in a variety of applications, demonstrating outstanding performance, often close to or above the human-level. Despite their success, some researchers have shown that neural networks can generalize poorly even with small data transformations (Azulay and Weiss 2018) as well as overfit to arbitrarily corrupted data (Zhang and Zhou 2017). Additionally, problems such as adversarial examples (Szegedy et al. 2013; Goodfellow, Shlens, and Szegedy 2014), which cause neural networks to misclassify slightly perturbed input data, can be a source of concern in real-world deployment of models. These challenges raise the question as to whether properties that enabled classical machine learning algorithms to overcome these problems can be useful in helping DNNs resolve similar problems. Specifically, (Schapire et al. 1998) introduced margin theory to explain boosting resistance to

over-fitting. Furthermore, the large margin principle, i.e., maximizing the smallest distance from the instances to the classification boundary in the feature space, has played an important role in theoretical analysis of generalization, and helped to achieve remarkable practical results (Cortes and Vapnik 1995), as well as robustness for input perturbations (Bousquet and Elisseeff 2001) on unseen data. Can the application of the large margin principle in DNNs lead to similar results?

Although computation of the actual margin in the input space of DNNs is intractable, studies show that the widely used cross-entropy loss function is by itself a proxy for converging to the maximal margin (Soudry et al. 2018). To date, this was only demonstrated for linear models that, similarly to SVM, have a theoretical guarantee for maximal margin convergence (Rosset, Zhu, and Hastie 2004). No such assurance for non-linear DNNs, their being highly non-convex, has been offered.

Recently, (Jiang et al. 2019) developed a measure for predicting the generalization gap¹ in DNNs that leverages *margin distribution*² (Garg, Har-Peled, and Roth 2002) as a more robust assessment for the margin notion in DNNs. In their work, they also point out that this measure can be used as an auxiliary loss function to achieve better generalization.

In the present study, we extend the aforementioned ideas and present a novel regularization term, which we denote as *Multi-Margin Regularization* (MMR), which can be added to any existing loss function in DNNs. We derive the regularization term starting from the binary case of large margin classification and generalize it to the multi-class case. This regularization term aims at increasing the margin induced by classifiers attained from the true class and its most competitive class. By summing over the margin distribution we compensate for class imbalance in the regularization term. Furthermore, due to the dynamic nature of feature space representation when training neural networks, we scale our formulation by the ever-changing maximal norm of the samples in the feature space, $\|\phi_{max}\|$.

We empirically show that applying this regularizer on the output layer of various DNNs, in different classification

¹The difference in accuracy between training and testing performance.

²The distribution of distances to the *decision boundaries*.

tasks and from different domains, is sufficient to obtain a substantial improvement in accuracy. In particular, we achieve valuable accuracy improvement in numerous image and text classification tasks, including CIFAR10, CIFAR100, ImageNet, MNLI, QQP and more.

In fact, our contribution is twofold. Alongside improving generalization performance using a new regularization scheme, we leverage the large margin principle to improve convergence during training using a selective-sampling scheme and assisted by a measure that we call the *Minimal Margin Score* (MMS). Essentially, MMS measures the distance to the decision boundary of the two most competitive predicted labels. This measure, in turn, is used to select, at the back-propagation pass, only those instances that accelerate convergence, thus speeding up the entire training process. It is worth noting that our selection criterion is based on computations that are an integral part of the forward pass, thus taking advantage of the "cheaper" inference computations. Lastly, we empirically show that using the MMS selection scheme with a faster learning-rate regime can improve, to a large extent, the convergence process.

1.1 Previous Approaches

The large margin principle has proven to be fundamentally important in the history of machine learning. While most of the efforts revolved around binary classification, extensions to multi-class classification were also suggested, e.g., multi-class perceptron (see Keslers construction, (Duda, Hart et al. 1973)), multi-class SVM (Vapnik 1998) and multi-class margin distribution (Zhang and Zhou 2017). Margin analysis have also been shown to correlate with better generalization properties (Schapire et al. 1998). Of particular interest to our study is the mistake-bound for multi-class linear separability that scales with $(R/\gamma)^2$, where R is the maximal norm of the samples in the feature space, and γ is the margin (Crammer and Singer 2003).

Computing the actual margin in DNNs, though, is intractable. (Soudry et al. 2018) proved that cross-entropy loss in linear DNNs, together with *stochastic gradient descent* (SGD) optimization, converges to a maximal margin solution, but it cannot ensure a maximal margin solution in non-linear DNNs. (Sun et al. 2015) affirmed that cross-entropy alone is not enough to achieve the maximal margin in DNNs and that an additional regularization term is needed.

Several works addressed the large margin principle in DNNs. (Elsayed et al. 2018) presented a multi-class linear approximation of the margin as an alternative loss function. They applied their margin-based loss at each and every layer of the neural network. Moreover, their method required a second order derivative computation due to the presence of first order gradients in the loss function itself. Explicit computation of the second order gradients for each layer of the neural network, however, can be quite expensive, especially when DNNs are getting wider and deeper. To address this limitation, they used a first order linear approximation to deploy their loss function more effectively. Later, (Jiang et al. 2019) presented a margin-based measure that strongly correlates with the generalization gap in DNNs. Essentially, they measured the difference between the training and the

test performances of a neural network using statistics of the marginal distribution (Garg, Har-Peled, and Roth 2002). (Sokolić et al. 2017) used the input layer to approximate the margin via the Jacobian matrix of the network and showed that maximizing their approximations leads to a better generalization. In contrast, we show that applying our margin-based regularization to the output layer alone achieves substantial improvements.

In addition to better generalization, we show that the large margin principle can also be used to accelerate the training of DNNs. Accelerating the training process is a long-standing challenge that has already been addressed by quite a few authors (Bengio and Senécal 2008; Salimans and Kingma 2016; Goyal et al. 2017). Specifically, we seek to highlight faster convergence via selective sampling. To date, the most notable sample selection approach is probably hard negative mining (Schroff, Kalenichenko, and Philbin 2015), where samples are selected by their loss values. The underlying assumption is that samples with higher losses have a significant impact on the model. Recent works employ selection schemes that examine the importance of the samples (Alain et al. 2015; Loshchilov and Hutter 2015). During training, the samples are selected based on their gradient norm, which in turn leads to a variance reduction in the stochastic gradients; see also (Katharopoulos and Fleuret 2018). Our selection method, though, utilizes uncertainty sampling, where the selection criterion is the proximity to the decision boundary, and we use the MMS measure to score the examples.

2 Margin Analysis for Binary and multi-class Classification

Consider a classification problem with two classes $\mathcal{Y} \in \{+1, -1\}$. We denote by $\mathcal{X} \in \mathcal{R}^d$ the input space. Let $f(\mathbf{w}^T \mathbf{x} + b)$ be a linear classifier, where $\mathbf{x} \in \mathcal{X}$ and

$$f(z) = \begin{cases} +1 & \text{if } z \geq 0 \\ -1 & \text{otherwise} \end{cases}$$

The classifier is trained using a set of examples $\{(\mathbf{x}_1, y_1), (\mathbf{x}_2, y_2), \dots, (\mathbf{x}_n, y_n)\} \in (\mathcal{X} \times \mathcal{Y})^m$ where each example is sampled identically and independently from an unknown distribution \mathcal{D} over $\mathcal{X} \times \mathcal{Y}$. The goal is to classify correctly new samples drawn from \mathcal{D} .

Denote by ℓ the (linear) decision boundary of the classifier

$$\ell = \{\mathbf{x} \mid \mathbf{w}^T \mathbf{x} + b = 0\} \quad (1)$$

The geometric distance of a point \mathbf{x} from ℓ is given by

$$d(\mathbf{x}) = \frac{\mathbf{w}^T \mathbf{x} + b}{\|\mathbf{w}\|} \quad (2)$$

For a linearly separable training set, there exist numerous consistent classifiers, i.e., classifiers that classify all examples correctly. Better generalization, however, is achieved by selecting the classifier that maximizes the margin \hat{d} ,

$$\arg \max_{\mathbf{w}, b} \hat{d} \quad \text{s.t.} \quad y_i \frac{\mathbf{w}^T \mathbf{x}_i + b}{\|\mathbf{w}\|} \geq \hat{d}, \quad \forall i = 1, \dots, m$$

This optimization is redundant with the length of \mathbf{w} and b . Imposing $y_i(\mathbf{w}^T \mathbf{x}_i + b) \geq 1$ removes this redundancy and results in the following equivalent minimization problem (Cortes and Vapnik 1995):

$$\min_{\mathbf{w}, b} \|\mathbf{w}\|^2 \quad \text{s.t.} \quad y_i(\mathbf{w}^T \mathbf{x}_i + b) \geq 1, \quad \forall i = 1, \dots, m$$

To handle noisy and linearly inseparable data, the set of linear constraints can be relaxed and substituted by the hinge loss,

$$\min_{\mathbf{w}, b} \|\mathbf{w}\|^2 + \lambda \sum_i \max(0, 1 - y_i(\mathbf{w}^T \mathbf{x}_i + b)) \quad (3)$$

The left term in Formula 3 is the *regularization* component and it promotes increasing of the margin between the data points and the decision boundary. The right term of the formula is the *empirical risk* component, imposing correct classifications on the training samples. The two terms employ two complementary forces; the former improves the generalization capability while the latter ensures the classification will be carried out correctly.

Next, we extend the large margin principle to the multi-class case. Let us assume we have a classification problem with n classes, $\mathcal{Y} \in \{1, \dots, n\}$, and a set of m training samples: $\{(\mathbf{x}_i, y_i)\} \in (\mathcal{X} \times \mathcal{Y})^m$. We now assign a score to each class: $s_i : \mathcal{X} \rightarrow \mathbb{R}, \forall i = 1..n$. For a linear classification, the j^{th} score of point i is:

$$s_j(\mathbf{x}_i) = \mathbf{w}_j^T \mathbf{x}_i + b_j$$

The predicted class is chosen by the maximal score attained over all classes,

$$\hat{y}_i = \arg \max_j s_j(\mathbf{x}_i)$$

For any two classes, $(p, q) \in \mathcal{Y} \times \mathcal{Y}$, the decision boundary between these classes is given by (see Figure 1):

$$\ell_{p,q} = \{\mathbf{x} \mid s_p(\mathbf{x}) = s_q(\mathbf{x})\} = \{\mathbf{x} \mid \mathbf{w}_p^T \mathbf{x} + b_p = \mathbf{w}_q^T \mathbf{x} + b_q\}.$$

Denoting $\mathbf{w}_{p,q} = \mathbf{w}_p - \mathbf{w}_q$ and $b_{p,q} = b_p - b_q$, the decision boundary $\ell_{p,q}$ can be rewritten as:

$$\ell_{p,q} = \{\mathbf{x} \mid \mathbf{w}_{p,q}^T \mathbf{x} + b_{p,q} = 0\}$$

which is similar to the binary case in Equation 1 where $\mathbf{w}_{p,q}$ replaces \mathbf{w} and $b_{p,q}$ replaces b . Similarly to Equation 2, the geometric distance of a point \mathbf{x} from $\ell_{p,q}$ is

$$d_{p,q}(\mathbf{x}) = \frac{\mathbf{w}_{p,q}^T \mathbf{x} + b_{p,q}}{\|\mathbf{w}_{p,q}\|} \quad (4)$$

For point \mathbf{x}_i , denote by $s_{y_i}(\mathbf{x}_i)$ the score for the true class and by $s_{m_i}(\mathbf{x}_i)$ the maximal score attained for the non-true classes, i.e., $m_i = \arg \max_{j \neq y_i} s_j(\mathbf{x}_i)$. Class m_i is the *competitive* class vis-à-vis y_i . The boundary decision between y_i and its competitive class is ℓ_{y_i, m_i} whose geometric distance to \mathbf{x}_i is

$$d_{y_i, m_i}(\mathbf{x}_i) = \frac{\mathbf{w}_{y_i, m_i}^T \mathbf{x}_i + b_{y_i, m_i}}{\|\mathbf{w}_{y_i, m_i}\|} \quad (5)$$

Note that $d_{y_i, m_i}(\mathbf{x}_i)$ is non-negative if the classification is correct ($s_{y_i}(\mathbf{x}_i) \geq s_{m_i}(\mathbf{x}_i)$) and negative otherwise.

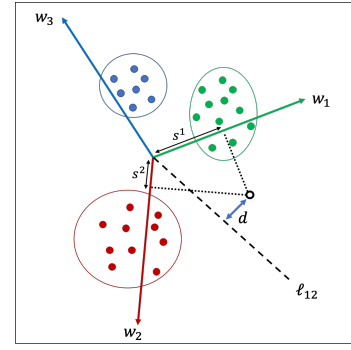


Figure 1: Illustrative example of a bi-class decision boundary.

For the multi-class case, Equation 3 can be generalized to the following optimization problem,

$$\min_{W, \mathbf{b}} \sum_i \|\mathbf{w}_{y_i, m_i}\|^2 + \lambda \sum_i \max(0, 1 - (\mathbf{w}_{y_i, m_i}^T \mathbf{x}_i + b_{y_i, m_i})) \quad (6)$$

where the optimization is over $W \doteq \{\mathbf{w}_1, \dots, \mathbf{w}_n\}$, and $\mathbf{b} \doteq \{b_1, \dots, b_n\}$. Here too, the left-hand term is the regularization penalty while the right-hand term represents the empirical risk with a hinge loss. The regularization term aims to increase the margin between the true class and its competitive class. Note, though, that the summation is over the margin distribution (i is the instance index). If the instances are evenly distributed over the classes, then this is equivalent to summation over the classes. Otherwise, this summation compensates for class imbalance in the regularization term.

3 Large Margin in DNNs

Applying the above scheme directly to DNNs poses several problems. First, these networks employ a non-linear mapping from the input space into a representation space: $\phi_i = F(\mathbf{x}_i, \theta) : \mathcal{X} \rightarrow \Phi$, where θ are the network parameters. The vector ϕ_i can be interpreted as a feature vector based on which the last layer in a DNN calculates the scores for each class via a fully-connected layer, $s_j(\phi_i) = \mathbf{w}_j^T \phi_i + b_j$. Maximizing the margin in the input space \mathcal{X} , as suggested in (Sokolić et al. 2017), requires back-propagating derivatives downstream the network up to the input layer, and calculating distances to the boundary up to the first order of approximation. In highly non-linear mappings, this approximation loses accuracy very fast as we move away from the decision boundary. Therefore, we apply the large margin principle in the last layer, where the distances to the decision boundary are Euclidean in the feature space Φ :

$$d_{y_i, m_i}(\phi_i) = \frac{\mathbf{w}_{y_i, m_i}^T \phi_i + b_{y_i, m_i}}{\|\mathbf{w}_{y_i, m_i}\|} \quad (7)$$

The second problem stems from the fact that in Equation 5 the input space \mathcal{X} is fixed along the course of training while the feature space Φ in Equation 7 is constantly changing. Accordingly, maximizing the margins in Equation 7 can be triv-

ially attained by scaling up the space Φ . Therefore, the feature space Φ must be constrained. In our scheme, we divide Equation 7 by $\|\phi_{max}\|$, the maximal norm of the samples in the feature space, of the current batch. This ensures that scaling up the feature space will not increase the distance in a free manner. The proposed formulation is translated, similarly to Equation 6, into the following optimization problem

$$\min_{W, b} \sum_i \mathcal{R}_i + \lambda \sum_i \mathcal{C}_i \quad (8)$$

where

$$\mathcal{R}_i = \|\mathbf{w}_{y_i, m_i}\|^2 \|\phi_{max}\|^2$$

denotes the margin regularization term, and \mathcal{C}_i is the empirical risk term. While for SVM, hinge loss is commonly used, in DNNs the common practice is to use cross-entropy

$$\mathcal{C}_i = -\log(P_{y_i})$$

where P_{y_i} is the probability of the true label y_i obtained from the network after the softmax layer:

$$P_{y_i} = \frac{e^{s_{y_i}(\mathbf{x}_i)}}{\sum_j e^{s_j(\mathbf{x}_i)}}$$

Similarly to hinge loss, cross-entropy will strive for correct classification while the regularization term will maximize the margin. For the rest of this paper we denote \mathcal{R}_i as the *multi-margin regularization* (MMR).

Note that the regularization term in this scheme is different from the weight decay commonly applied in deep networks. First, here, the minimization is applied over the \mathbf{w} differences of: $\|\mathbf{w}_{y_i, m_i}\|^2 = \|\mathbf{w}_{y_i} - \mathbf{w}_{m_i}\|^2$. Additionally, the regularization term is multiplied by the $\|\phi_{max}\|$. Lastly, the regularization term is implemented only at the last layer.

4 Accelerating Training Using Minimal Margin Score Selection

We continue to leverage the principle of large margin in neural networks to address the computational limitations in real-world applications, specifically in the selective sampling scheme. We show that by selecting samples that are closer to the margin in the multi-class setting during the forward pass, we achieve better convergence and speed-up during the training process. To this end, we evaluate our suggested method on CIFAR10 and CIFAR100 using ResNet-44 (He et al. 2016) and WRN-28-10 (Zagoruyko and Komodakis 2016) architectures. To demonstrate the effectiveness of our selection more vigorously, we apply a faster learning-rate (LR) regime than those suggested in the original papers.

In principle, our selection method is based on the evaluation of the minimal amount of displacement a training sample should undergo until its predicted classification is switched. We call this measure the *minimal margin score* (MMS). This measure depends on the highest and the second highest scores achieved per sample. Similarly to our margin-based regularization, we apply our measure only to the output layer, and calculate it linearly with respect to the input of the last layer. Additionally, unlike (Jiang et al. 2019), we

do not take into consideration the true label, i.e., our measure is calculated based solely on the highest and the second highest neural network scores.

As shown in Figure 1, a multi-class classification problem is composed of three classes, Green, Red, and Blue, along with three linear projections, $\mathbf{w}_1, \mathbf{w}_2$, and \mathbf{w}_3 , respectively. The query point is marked by an empty black circle. The highest scores of the query point are s^1 and s^2 (assuming all biases are 0's), where $s^1 > s^2$ and s^3 are negative (not marked). Since the two highest scores are for the Green and Red classes, the distance of the query point to the decision boundary between these two classes is d . The magnitude of d is the MMS of this query point.

Formally, let $\mathcal{X} = \{\mathbf{x}_1, \dots, \mathbf{x}_m\}$ be a large set of samples and $\phi_i = F(\mathbf{x}_i; \theta) \in \Phi$ be the input to the last layer of the neural network. Assume we have a classification problem with n classes. At the last layer, the classifier s consists of n linear functions: $s_j : \phi \rightarrow \mathbb{R}$ for $j = 1 \dots n$ where s_j is a linear mapping $s_j(\phi) = \mathbf{w}_j^T \phi + b_j$. Denote the sorted scores of $\{s_j(\phi_k)\}_{j=1}^n$ by $\mathcal{S} = (s_k^{j_1}, s_k^{j_2}, \dots, s_k^{j_n})$, where $s_k^{j_p} \geq s_k^{j_{p+1}}$ and $s_k^{j_p} = s_{j_p}(\phi_k)$. The classifier $s_{j_1}(\phi_k)$ gives the highest score and $s_{j_2}(\phi_k)$, the second highest score. The *decision boundary* between classes j_1 and j_2 is defined as:

$$\ell_{12} = \{\phi \mid s_{j_1}(\phi) = s_{j_2}(\phi)\}$$

Using this definition, the confidence of the predicted label j_1 of point ϕ_k is determined by the distance d_k of ϕ_k to the decision boundary ℓ_{12} . Following Equation 7, it is easy to show that

$$d_k = \frac{s_k^{j_1} - s_k^{j_2}}{\|\mathbf{w}_{j_1} - \mathbf{w}_{j_2}\|} \quad (9)$$

The distance d_k is the MMS of point \mathbf{x}_k . The larger d_k , the more confident we are about the predicted label. Conversely, the smaller d_k , the less confident we are about the predicted label j_1 . Therefore, d_k can serve as a confidence measure for the predicted labels. Accordingly, the best points to select for the back-propagation step are the points whose MMS are the smallest. Note that in contrast to the MMR, in this case we do not have to normalize the distance d_k with $\|\phi_{max}\|$ because this normalization will not change the order of \mathcal{S} , and thus the set of selected points will remain unchanged.

Our implementation consists of a generic, yet simple, on-line selective sampling method, applied at the beginning of each training step. Specifically, at each training step, we first apply a forward pass on a batch of points of size B , and obtain their respective scores. We then calculate their respective MMS measures, and select the b samples ($b \ll B$) whose MMS measures are the smallest. The resulting batch of size b , in turn, is used for training the network. The selection process is repeated every training step, thus potentially selecting a new batch of points for training. The MMS-based training procedure is summarized in Algorithm 1.

5 Experiments

In this section³, we report on the series of experiments we designed to evaluate the MMR's ability to achieve a higher

³All experiments were conducted using PyTorch; the code will be released on github upon acceptance of the paper.

Algorithm 1: MMS-based training

Require: Inputs $\mathcal{X} = \{\mathbf{x}_i\}_{i=1}^B, F(\cdot; \theta_0)$

- 1: $t \leftarrow 1$
- 2: **repeat**
- 3: $\Phi \leftarrow F(\mathcal{X}; \theta_{t-1})$ forward pass a batch of size B
- 4: $MMS \leftarrow d(\Phi)$ calc. MMS
- 5: $S \leftarrow \text{sort_index}(MMS, b)$ store b smallest scores
- 6: $\mathcal{X}_b = \{\mathbf{x}_i | i \in S\}$ subset of \mathcal{X} of size b
- 7: $\theta_t \leftarrow \text{sgd_step}(F(\mathcal{X}_b; \theta_{t-1}))$ back prop. batch of size b
- 8: $t \leftarrow t + 1$
- 9: **until** reaching final model accuracy

accuracy score, and the MMS selection method’s ability to achieve a faster convergence than the original training algorithms (the baseline) and data augmentation. The experiments were conducted on commonly used datasets and neural network models, in the vision and *natural language processing* (NLP) realms.

Our experimental workbench is composed of CIFAR10, CIFAR100 (Krizhevsky, Hinton et al. 2009) and ImageNet (Deng et al. 2009) for image classification; Question NLI (QNLI) (Wang et al. 2018), MultiNLI (MNLI) (Williams, Nangia, and Bowman 2017) and Recognizing Textual Entailment (RTE) (Bentivogli et al. 2009) for natural language inference; MSR Paraphrase Corpus (MRPC) (Dolan and Brockett 2005) and Quora Question Pairs (QQP) (Chen et al. 2018) for sentence similarity; Stanford Sentiment Treebank-2 (SST-2) (Socher et al. 2013) for text classification.

5.1 Image Classification

CIFAR10 and CIFAR100. These are image classification datasets that consist of 32×32 color images from 10 or 100 classes, consisting of 50k training examples and 10k test examples. The last 5k images of the training set are used as a held-out validation set, as suggested in common practice. For our experiments, we used ResNet-44 (He et al. 2016) and WRN-28-10 (Zagoruyko and Komodakis 2016) architectures. We applied the original hyper parameters and training regime using a batch-size of 64. In addition, we used the original augmentation policy as described in (He et al. 2016) for ResNet-44, while adding cutout (DeVries and Taylor 2017) and auto-augment (Cubuk et al. 2018) for WRN-28-10. Optimization was performed for 200 epochs (equivalent to 156K iterations) after which baseline accuracy was obtained with no apparent improvement.

ImageNet. For large-scale evaluation, we used the ImageNet dataset (Deng et al. 2009), containing more than 1.2M images in 1k classes. In our experiments, we used MobileNet (Howard et al. 2017) architecture and followed the training regime established by (Goyal et al. 2017) in which an initial LR of 0.1 is decreased by a factor of 10 in epochs 30, 60, and 80, for a total of 90 epochs. We used a base batch size of 256 over four devices and L_2 regularization

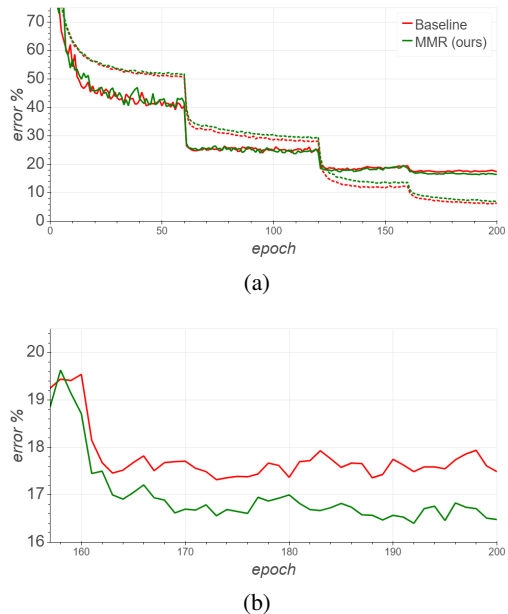


Figure 2: Training (dashed) and validation errors of CIFAR100 using the WRN28-10 neural network and comparing baseline training and our MMR approach. We use linear scale α , starting with $1e - 5$ up to $1e - 3$.

over weights of convolutional layers as well as the standard data augmentation.

Improving accuracy via MMR

The MMR was added to the objective function as an additional regularization term, where α is a trade-off factor between the cross-entropy loss and the regularization ⁴:

$$\mathcal{L}(\theta) = \alpha \sum_i \mathcal{R}_i + \sum_i \mathcal{C}_i$$

To find the optimal α , we used a grid search and found that a linear scaling of α in the range of $[1e - 5..1e - 3]$ works best for CIFAR10/100 and static $\alpha = 1e - 5$ works best for ImageNet.

Table 1 demonstrates our final results when increasing the final model’s accuracy on CIFAR10 and CIFAR100. Specifically, we managed to improve baseline accuracy in ResNet-44 from 93.22% to 93.83% and from 93.19% to 93.34% in VGG. We also see a relative change in error of 9.00% and 2.20%, respectively, on the CIFAR10 dataset. Furthermore, we show a substantial decrease of 5.77% in the error for CIFAR100 using the WRN-28-20 model (see Figure 2), raising its absolute accuracy by more than 1%. Altogether, we observed a 2.67% average decrease in error on all datasets.

Convergence speedup via MMS selective sampling

To test our hypothesis that using the MMS selection method we could accelerate training while preserving final model

⁴This formulation is equivalent to Equation 8, where $\alpha = \frac{1}{\lambda}$. It is preferred because it leads to multiplying the regularization term by a small number and keeping the scaling factor of \mathcal{C}_i to be 1, thus avoiding gradient enlargement.

Model	Dataset	Baseline	Our MMR	Change
ResNet-44 (He et al. 2016)	CIFAR10	93.22%	93.83%	9.00%
VGG (Simonyan and Zisserman 2014)	CIFAR10	93.19%	93.34%	2.20%
WRN-28-10 + auto-augment + cutout (Zagoruyko and Komodakis 2016)	CIFAR100	82.51%	83.52%	5.77%
VGG + auto-augment + cutout	CIFAR100	73.93%	74.19%	1.00%
MobileNet (Howard et al. 2017)	ImageNet	71.17%	71.44%	0.94%
BERT _{BASE} (Devlin et al. 2018)	QNLI	91.06%	91.48%	4.70%
	SST-2	92.08%	92.43%	4.42%
	MRPC	90.68%	91.43%	8.05%
	RTE	68.23%	69.67%	4.53%
	QQP	87.9%	88.04%	1.16%
	MNLI	84.5%	84.70%	1.29%

Table 1: Test accuracy results. Top1 for CIFAR10/100 datasets. Any relative change in error over the baseline is listed in percentage, and improvements higher than 4% are marked in bold. F1 scores are reported for QQP and MRPC. For MNLI, we report the average of the matched (with $\alpha = 1e - 5$) and miss-matched (with $\alpha = 1e - 6$) for both the baseline and our MMR.

accuracy, we designed a new, more aggressive leaning-rate drop regime than the one used by the authors of the original paper. Figure 3 presents empirical evidence supporting our hypothesis. We compared the results of our MMS method against random selection⁵, and against *hard-negative mining* that prefers samples with low prediction scores (Yu et al. 2018; Schroff, Kalenichenko, and Philbin 2015). For the latter, we used the implementation suggested by (Hoffer et al. 2018), termed "NM-sample", where the cross-entropy loss is used for the selection.

For CIFAR10 and ResNet-44, we used the original LRs $\eta = \{0.1, 0.01, 0.001, 0.0001\}$ while decreasing them at steps $\{24992, 27335, 29678\}$, equivalent to epochs $\{32, 35, 38\}$ with a batch of size 64. As depicted in Figure 3 (top), we can see that our selection method indeed yields validation accuracy extremely close to the one reached by the baseline training scheme, with considerably fewer training steps. Specifically, we reached 93% accuracy after merely 44K steps (a minor drop of 0.25% compared to the baseline). We also applied the early drop regime to the baseline configuration as well as to the NM-samples. Both failed to reach the desired model accuracy while suffering from a degradation of 1.57% and 1.22%, respectively.

Similarly, we applied the early LR drop scheme for CIFAR100 and WRN-28-10, using $\eta = \{0.1, 0.02, 0.004, 0.0008\}$ and decreasing steps $\{39050, 41393, 43736\}$ equivalent to epochs $\{50, 53, 56\}$, with batch of size 64. As depicted in Figure 3 (bottom), MMS accuracy reached 82.2% with a drop of 0.07% compared to the baseline, while almost halving the number of steps (80K vs. 156K). On the other hand, the baseline and the NM-sample schemes failed to reach the desired accuracy after we applied a similar early drop regime. For the NM-sample approach, the degradation was the most significant, with a drop of 2.97% compared to the final model accuracy, while the baseline drop was approximately 1%.

⁵Referred to as baseline with and without an early LR drop.

These results are in line with the main theme of selective sampling that strives to focus training on more informative points. Training loss, however, can be a poor proxy for this concept. For example, the NM-sample selection criterion favors high loss scores, which obviously increases the training error, while our MMS approach selects uncertain points, some of which might be correctly classified. Others might be mis-classified by a small margin, but they are all close to the decision boundary, and hence useful for training.

5.2 Natural Language Classification Tasks

To challenge our premise that we could achieve a higher accuracy score, we examined our MMR on an NLP-related model and datasets. In particular, we used the BERT_{BASE} model (Devlin et al. 2018) with 12 transformer layers, a hidden dimensional size of 768 and 12 self-attention heads. Fine-tuning was performed using the Adam optimizer as in the pre-training, with a dropout probability of 0.1 on all layers. Additionally, we used a LR of $2e - 5$ over three epochs in total for all the tasks. We used the original WordPiece embeddings (Wu et al. 2016) with a 30k token vocabulary. For our method, similarly to the image classification task, we also used the α factor in the objective function, and found via a grid search, $\alpha = 1e - 5$ to be the optimal⁶.

We performed experiments on a variety of supervised tasks, specifically by applying downstream task fine-tuning on natural language inference, semantic similarity, and text classification. All these tasks are available as part of the GLUE multi-task benchmark (Wang et al. 2018).

Natural Language Inference The task of natural language inference (NLI) or recognizing textual entailment means that when a pair of sentences is given, the classifier decides whether or not they contradict each other. Although there has been a lot of progress, the task remains challenging due to the presence of a wide variety of phenomena such as lexical entailment, coreference, and lexical and syntactic

⁶We applied $\alpha = 1e - 6$ only to evaluate our method's accuracy with the miss-matched MNLI.

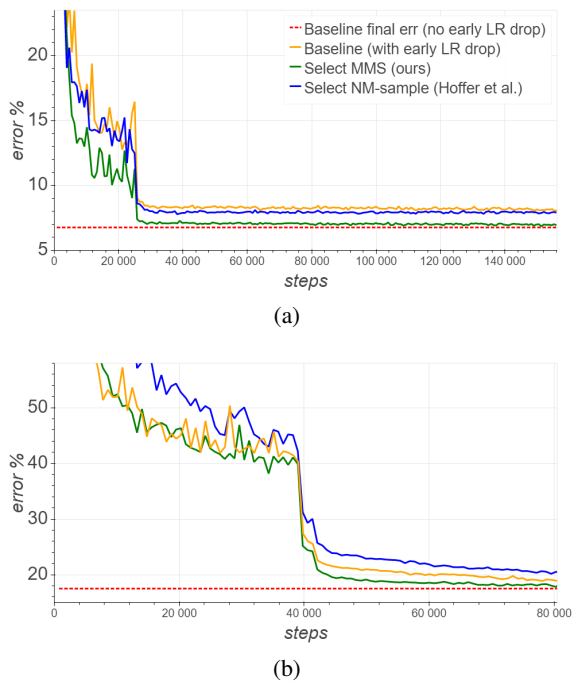


Figure 3: Validation errors of ResNet44, CIFAR10 (top) and WRN-28-10, CIFAR100 (bottom). We compared the baseline training, NM-sample selection (hard negative mining), and MMS (our) selection method using a faster regime. We plotted the regular regime baseline’s final errors as a dotted line for perspective. **The MMS selection method achieves on par final test accuracy using fewer numbers of training steps.**

ambiguity. We evaluate our scheme on three NLI datasets taken from different sources, including transcribed speech, popular fiction, and government reports (MNLI), Wikipedia articles (QNLI) and news articles (RTE).

As shown in Table 1, our scheme using the regularization term outperformed baseline results on all the three tasks. We achieved absolute improvement of up to 1.44% on RTE and a relative change in error of 4.53%. On QNLI and MNLI we also achieved higher scores of 91.48% (accuracy) and 84.70% (F1), outperforming the baseline results by 0.42% and 0.2%, respectively.

Semantic Similarity This task involves predicting whether two sentences are semantically equivalent by identifying similar concepts in both sentences. It can be challenging for a language model to recognize syntactic and morphological ambiguity as well as compare the same ideas using different expressions or the other way around. We evaluated our approach on QQP and MRPC downstream tasks, outperforming baseline results as can be seen in Table 1. On MRPC in particular, we achieved a relative change of more than 8%.

Text Classification Lastly, we evaluated our method on the Stanford Sentiment Treebank (SST-2), which is a binary single-sentence classification task consisting of sentences extracted from movie reviews with human annotations of their sentiment. Our approach outperformed the baseline by a relative error change of 4.42%.

Overall, applying MMR boosted the accuracy in all the reported tasks. This indicates that our approach works well for different tasks from various domains.

6 Discussion

We studied a multi-class margin analysis for DNNs and use it to devise a novel regularization term, the *multi-margin regularization* (MMR). Similarly to previous formulations, the MMR aims at increasing the margin induced by the classifiers, and it is derived directly, for each sample, from the true class and its most competitive class. The main difference between the MMR and common regularization terms is that MMR is scaled by $\|\phi_{max}\|$, which is the maximal norm of the samples in the feature space. This ensures a meaningful increase in the margin that is not induced by a simple scaling of the feature space. Additionally, weight differences are minimized rather than the commonly used determinant or other norms of W . Lastly, MMR is formulated and performed over the margin distribution to compensate for class imbalance in the regularization term. The MMR can be incorporated with any empirical risk loss and it is not restrictive to hinge loss or cross-entropy losses. And indeed, using MMR, we demonstrate improved accuracy over a set of experiments in images and text.

Additionally, the multi-class margin analysis enables us to propose a selective sampling method designed to accelerate the training of DNNs. Specifically, we utilized uncertainty sampling, where the criterion for selection is the distance to the decision boundary. To this end, we introduced a novel measurement, the *minimal margin score* (MMS), which measures the minimal amount of displacement an input should undergo until its predicted classification is switched. For multi-class linear classification, the MMS measure is a natural generalization of the margin-based selection criterion.

Our selection criterion was inspired by the active learning method, but our goal, to accelerate training, is different. Active learning is mainly concerned with labeling cost. Hence, it is common to keep on training until convergence, before turning to select additional examples to label. When the goal is merely acceleration, labeling cost is not a concern, and one can adapt a more aggressive protocol and re-select a new batch of examples at each training step.

The MMS measure does not use the labels. Thus, it can be used to select samples in an active learning setting as well. Similarly to (Jiang et al. 2019) the MMS measure can be implemented at other layers in the deep architecture. This enables selection of examples that directly impact training at all levels. The additional computation associated with such a framework makes it less appealing for the purpose of acceleration. For active learning, however, it may introduce an additional gain. The design of a novel active learning method is left for further study.

References

- Alain, G.; Lamb, A.; Sankar, C.; Courville, A.; and Bengio, Y. 2015. Variance reduction in sgd by distributed importance sampling. *arXiv preprint arXiv:1511.06481* .
- Azulay, A.; and Weiss, Y. 2018. Why do deep convolutional networks generalize so poorly to small image transformations? *arXiv preprint arXiv:1805.12177* .
- Bengio, Y.; and Senécal, J.-S. 2008. Adaptive importance sampling to accelerate training of a neural probabilistic language model. *IEEE Transactions on Neural Networks* 19(4): 713–722.
- Bentivogli, L.; Clark, P.; Dagan, I.; and Giampiccolo, D. 2009. The Fifth PASCAL Recognizing Textual Entailment Challenge. In *TAC*.
- Bousquet, O.; and Elisseeff, A. 2001. Algorithmic stability and generalization performance. In *Advances in Neural Information Processing Systems*, 196–202.
- Chen, Z.; Zhang, H.; Zhang, X.; and Zhao, L. 2018. Quora question pairs.
- Cortes, C.; and Vapnik, V. 1995. Support-vector networks. *Machine learning* 20(3): 273–297.
- Crammer, K.; and Singer, Y. 2003. Ultraconservative online algorithms for multiclass problems. *Journal of Machine Learning Research* 3(Jan): 951–991.
- Cubuk, E. D.; Zoph, B.; Mane, D.; Vasudevan, V.; and Le, Q. V. 2018. Autoaugment: Learning augmentation policies from data. *arXiv preprint arXiv:1805.09501* .
- Deng, J.; Dong, W.; Socher, R.; Li, L.-J.; Li, K.; and Fei-Fei, L. 2009. ImageNet: A Large-Scale Hierarchical Image Database. In *2009 IEEE conference on computer vision and pattern recognition*, 248–255.
- Devlin, J.; Chang, M.-W.; Lee, K.; and Toutanova, K. 2018. Bert: Pre-training of deep bidirectional transformers for language understanding. *arXiv preprint arXiv:1810.04805* .
- DeVries, T.; and Taylor, G. W. 2017. Improved regularization of convolutional neural networks with cutout. *arXiv preprint arXiv:1708.04552* .
- Dolan, W. B.; and Brockett, C. 2005. Automatically constructing a corpus of sentential paraphrases. In *Proceedings of the Third International Workshop on Paraphrasing (IWP2005)*.
- Duda, R. O.; Hart, P. E.; et al. 1973. *Pattern classification and scene analysis*. Wiley New York.
- Elsayed, G.; Krishnan, D.; Mobahi, H.; Regan, K.; and Bengio, S. 2018. Large margin deep networks for classification. In *Advances in neural information processing systems*, 842–852.
- Garg, A.; Har-Peled, S.; and Roth, D. 2002. On generalization bounds, projection profile, and margin distribution. In *ICML*, 171–178.
- Goodfellow, I. J.; Shlens, J.; and Szegedy, C. 2014. Explaining and harnessing adversarial examples. *arXiv preprint arXiv:1412.6572* .
- Goyal, P.; Dollár, P.; Girshick, R.; Noordhuis, P.; Wesolowski, L.; Kyrola, A.; Tulloch, A.; Jia, Y.; and He, K. 2017. Accurate, large minibatch sgd: Training imagenet in 1 hour. *arXiv preprint arXiv:1706.02677* .
- He, K.; Zhang, X.; Ren, S.; and Sun, J. 2016. Deep residual learning for image recognition. In *Proceedings of the IEEE conference on computer vision and pattern recognition*, 770–778.
- Hoffer, E.; Weinstein, B.; Hubara, I.; Gofman, S.; and Soudry, D. 2018. Infer2Train: leveraging inference for better training of deep networks. *NeurIPS 2018 Workshop on Systems for ML* .
- Howard, A. G.; Zhu, M.; Chen, B.; Kalenichenko, D.; Wang, W.; Weyand, T.; Andreetto, M.; and Adam, H. 2017. Mobilenets: Efficient convolutional neural networks for mobile vision applications. *arXiv preprint arXiv:1704.04861* .
- Jiang, Y.; Krishnan, D.; Mobahi, H.; and Bengio, S. 2019. Predicting the generalization gap in deep networks with margin distributions. In *7th International Conference on Learning Representations, ICLR*. URL <https://openreview.net/pdf?id=HJIQfnCqKX>.
- Katharopoulos, A.; and Fleuret, F. 2018. Not all samples are created equal: Deep learning with importance sampling. *arXiv preprint arXiv:1803.00942* .
- Krizhevsky, A.; Hinton, G.; et al. 2009. Learning multiple layers of features from tiny images. Technical report, Cite-seer.
- Loshchilov, I.; and Hutter, F. 2015. Online batch selection for faster training of neural networks. *arXiv preprint arXiv:1511.06343* .
- Rosset, S.; Zhu, J.; and Hastie, T. J. 2004. Margin maximizing loss functions. In *Advances in neural information processing systems*, 1237–1244.
- Salimans, T.; and Kingma, D. P. 2016. Weight normalization: A simple reparameterization to accelerate training of deep neural networks. In *Advances in neural information processing systems*, 901–909.
- Schapire, R. E.; Freund, Y.; Bartlett, P.; Lee, W. S.; et al. 1998. Boosting the margin: A new explanation for the effectiveness of voting methods. *The annals of statistics* 26(5): 1651–1686.
- Schroff, F.; Kalenichenko, D.; and Philbin, J. 2015. Facenet: A unified embedding for face recognition and clustering. In *Proceedings of the IEEE conference on computer vision and pattern recognition*, 815–823.
- Simonyan, K.; and Zisserman, A. 2014. Very deep convolutional networks for large-scale image recognition. *arXiv preprint arXiv:1409.1556* .
- Socher, R.; Perelygin, A.; Wu, J.; Chuang, J.; Manning, C. D.; Ng, A. Y.; and Potts, C. 2013. Recursive deep models for semantic compositionality over a sentiment treebank. In *Proceedings of the 2013 conference on empirical methods in natural language processing*, 1631–1642.

- Sokolić, J.; Giryas, R.; Sapiro, G.; and Rodrigues, M. R. 2017. Robust large margin deep neural networks. *IEEE Transactions on Signal Processing* 65(16): 4265–4280.
- Soudry, D.; Hoffer, E.; Nacson, M. S.; Gunasekar, S.; and Srebro, N. 2018. The implicit bias of gradient descent on separable data. *The Journal of Machine Learning Research* 19(1): 2822–2878.
- Sun, S.; Chen, W.; Wang, L.; and Liu, T. 2015. Large Margin Deep Neural Networks: Theory and Algorithms. *ArXiv abs/1506.05232*.
- Szegedy, C.; Zaremba, W.; Sutskever, I.; Bruna, J.; Erhan, D.; Goodfellow, I. J.; and Fergus, R. 2013. Intriguing properties of neural networks. *arXiv preprint arXiv:1312.6199* .
- Vapnik, V. 1998. *Statistical learning theory*. Wiley New York.
- Wang, A.; Singh, A.; Michael, J.; Hill, F.; Levy, O.; and Bowman, S. R. 2018. Glue: A multi-task benchmark and analysis platform for natural language understanding. *arXiv preprint arXiv:1804.07461* .
- Williams, A.; Nangia, N.; and Bowman, S. R. 2017. A broad-coverage challenge corpus for sentence understanding through inference. *arXiv preprint arXiv:1704.05426* .
- Wu, Y.; Schuster, M.; Chen, Z.; Le, Q. V.; Norouzi, M.; Macherey, W.; Krikun, M.; Cao, Y.; Gao, Q.; Macherey, K.; et al. 2016. Google’s neural machine translation system: Bridging the gap between human and machine translation. *arXiv preprint arXiv:1609.08144* .
- Yu, H.; Zhang, Z.; Qin, Z.; Wu, H.; Li, D.; Zhao, J.; and Lu, X. 2018. Loss Rank Mining: A General Hard Example Mining Method for Real-time Detectors. In *2018 International Joint Conference on Neural Networks (IJCNN)*, 1–8. IEEE.
- Zagoruyko, S.; and Komodakis, N. 2016. Wide residual networks. *arXiv preprint arXiv:1605.07146* .
- Zhang, T.; and Zhou, Z.-H. 2017. Multi-class optimal margin distribution machine. In *International Conference on Machine Learning*, 4063–4071.